

Relationship between Radon and the Tectonic Activity of Faults in Central Mongolia

K. Zh. Seminsky^{a,*}, A. A. Bobrov^a, and S. Demberel^b

Presented by Academician Yu.M. Pushcharovskii August 28, 2017

Received December 29, 2017

Abstract—The relationship between radon and the tectonic activity of faults for two geodynamically active regions of Central Mongolia is shown with account for the influence of individual characteristics of the radon field. As a whole, the radon activity of the faults increases with an increasing contribution of extension to the dynamic environment of their formation, with increasing seismic activity, and near concentrated faults of the late stages of evolution in comparison with the wide zones of fractures at the early stages of the formation of the internal structure. The studied patterns should provide an increase in the efficiency of application of radon surveys in investigation of the seismic hazard of faults in the Earth's crust.

DOI: 10.1134/S1028334X19080166

INTRODUCTION

The problem of the relationship of radon and the tectonic activity of faults is one of the most complex in geodynamics due to the high sensitivity of gas emanations to the various inner and outer influences on the Earth. At the same time, the contribution of internal deforming forces to the formation of a radon field predominates for tectonically active regions, in the geochemical environments with a standard U concentration, because these forces determine the dynamics of the stress state of the upper crust, which causes the release of radioactive gas into the atmosphere ([1, 5, 9, 10] and others). With regard to the practical importance of estimation of the tectonic activity and seismic hazards of faults, this is one of the major reasons for the increase in the number of publications on the radon activity of faults and the relationship between gas emanations and seismicity in recent years.

In this paper, we consider the relationship between radon and the tectonic activity of faults for two regions of central Mongolia. This is the region of the strong Mogod earthquake ($M = 7.8$, January 5, 1967), as well as the neighboring areas of Ulaanbaatar, where seismic activity has increased in recent years. In contrast

to previous studies [9], here we analyze the influence of the main characteristics of the fault reflecting its tectonic activity directly or indirectly by radon emanations. These are the dynamic environment of the formation of the fault (compression, strike-slip etc.), its rank, state of the internal structure, and the seismic activity, which, in the absence of the data on the motion rates, is the first approximation to the intensity of modern displacements.

The objects of this study included ten dislocations (Fig. 1a); five of them were represented by the faults of the Ulaanbaatar area (Skai, Sherkhai, Avdar, Gunzhin, and Emeelt) and five rectilinear segments of large disjunctives that have been allocated for study as separate structures due to the difference in orientation and/or dynamic environment of the formation. These are the multi-oriented segments of the Khustai Fault (1, 2, and 3) in the vicinity of the Mongolian capital; the meridional strike-slip (Mogod) and the north-westerly reverse (Tulet) branches of the seismic rupture formed in 1967, in the Mogodskaya area.

The dynamic setting of the formation of the faults studied was determined by others [4, 6, 7]. The rank was estimated by the total length of relief terraces (Fig. 1a) or soil dislocations formed as a result of displacements along the fault. As a whole, the objects studied are subdivided into two groups, and the length of the second-rank faults (~40 km) is two times higher than the length of the first-rank dislocations (~20 km). The seismic activity of dislocations was estimated by the distribution of earthquake epi-

^a Institute of the Earth's Crust, Siberian Branch, Russian Academy of Sciences, Irkutsk, 664033 Russia

^b Institute of Astronomy and Geophysics, Mongolian Academy of Sciences, Ulaanbaatar, Mongolia

*e-mail: seminsky@crust.irk.ru

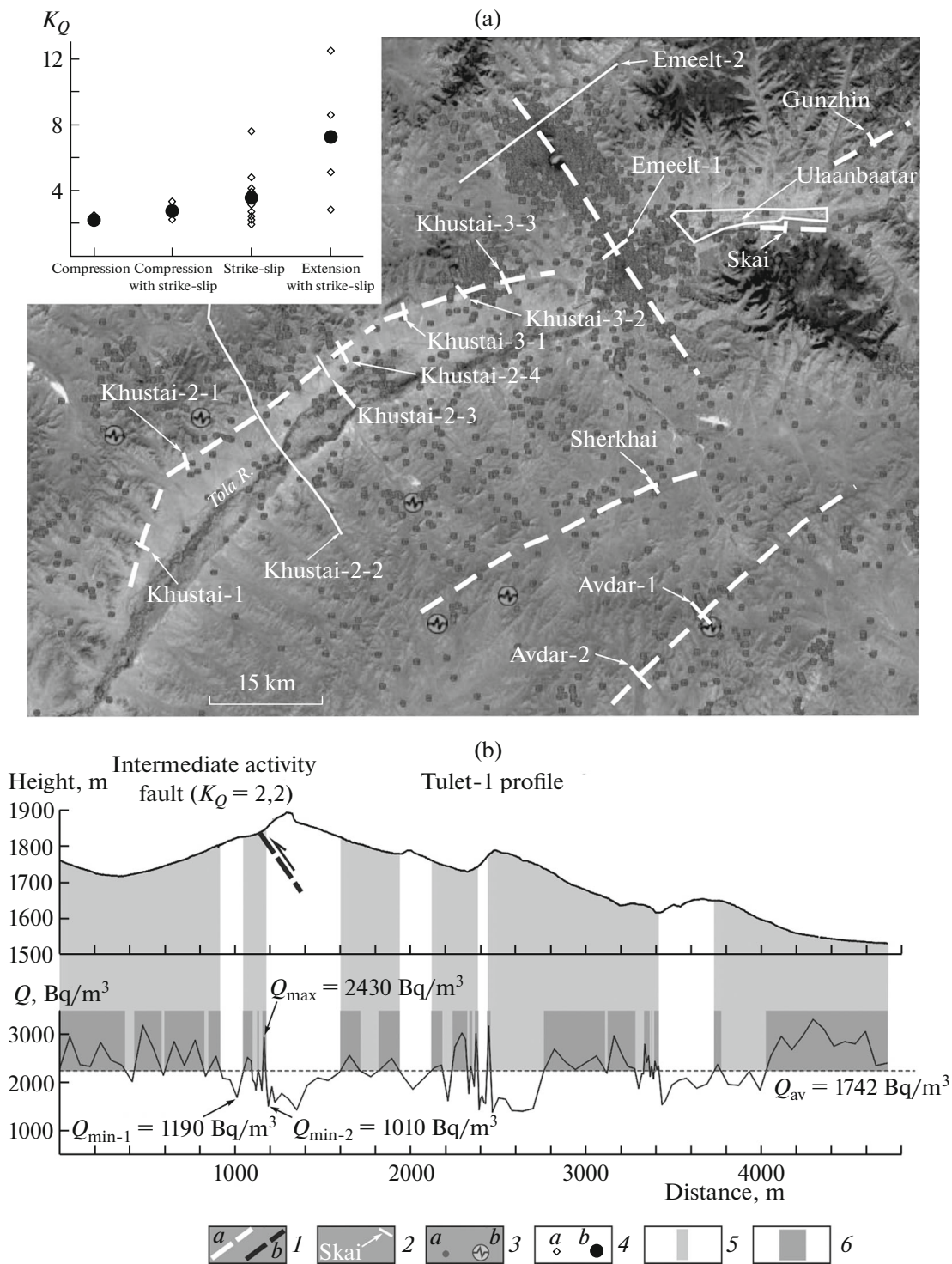


Fig. 1. Scheme of the profiles of the emanation survey in the area of Ulaanbaatar (a) and the results of radon monitoring for one of the profiles within the Mogod area (b). (a) Location of the earthquake epicenters (2000–2014), major faults, and emanation profiles on the space image. The inset shows the diagram of the influence of the dynamic environment of fault formation on its radon activity coefficient K_Q ; (b) variation in the absolute heights (top) and bulk activity of soil radon Q (bottom) along the Tulet-1 profile crossing the major strike-slip of the reverse branch of the seismic rupture formed in 1967 during the Mogod earthquake ($M = 7.8$). (1) Faults on the scheme (a) and profile (b); (2) location and names of the profiles; (3) epicenters of earthquakes with a magnitude of <3 (a) and >3 (b); (4) near-fault radon anomalies; (5) areas of the profile with anomalous concentrations of soil radon ($Q > Q_{av}$). Q_{max} , Q_{min-1} , and Q_{min-2} are the parameters of the radon anomaly applied in calculations of K_Q for the seismic rupture Tulet-1.

centers (Fig. 1a), which were poor ($M = 0.5\text{--}4.5$) in the period of emanation studies and accompanied the formation of all objects studied, except for the Skai and Khustai-1 faults.

The methodology of this study is described in detail in [9]. To estimate the radon activity of the objects studied, we carried out emanation monitoring, which included measurement of the bulk activity of soil radon (Q , Bq/m³) at individual points of the profiles crossing each of the faults (Fig. 1a). Based on the results of measurements, the relative coefficient of radon activity (K_Q) was determined for each fault:

$$K_Q = Q_{\max}/Q_{\min},$$

where Q_{\max} is the intensity of the near-fault anomaly; Q_{\min} is the minimal value of Q directly outside its boundaries ($Q_{\min} = (Q_{\min-1} + Q_{\min-2})/2$ (Fig. 1b)).

K_Q is less dependent on the meteorological conditions and radioactivity of rocks in comparison with Q_{\max} and is mostly controlled by the structure of the fault zone and the degree of its tectonic activity. Based on the K_Q value, the faults of ultrahigh ($K_Q > 10$), very high ($10 \geq K_Q > 5$), high ($5 \geq K_Q > 3$), intermediate ($3 \geq K_Q > 2$), and low ($K_Q \leq 2$) radon activity are distinguished [9].

In addition to the contrast (K_Q) and intensity (Q_{\max}), the width (H) was determined for each fault anomaly. The values of $Q > Q_{\text{av}}$, where Q_{av} is the average from all values measured along the profile (Fig. 1b), were considered as anomalous. The small sections of the profile with $Q < Q_{\text{av}}$ were included in the boundaries of the anomaly if they were located between two anomalous domains and had a smaller size than at least one of them.

Analysis of the results of emanation monitoring is based on study of the characteristics mentioned obtained for each fault (in the case of several intersections, the data was averaged).

The width of near-fault radon anomalies for the faults of various ranks ranges within 80–1625 m, while the intensity of near-fault anomalies (Q_{\max}) is 2525–9298 Bq/m³. K_Q varies from 1.9 to 7.6 and allows us to allocate the studied faults to four groups characterized by the ultrahigh (Khustai-2 and Skai), high (Khustai-3, Sherkhai, Avdar, and Gunzhin), intermediate (Emelt, Mogod, and Tulet), and low (Khustai-1) radon activity.

The dynamic environment of fault formation affects significantly its radon activity increasing in the following series: compression–compression with strike-slip–strike-slip–extension with strike-slip (see inset in Fig. 1a), i.e., with an increasing contribution of extension and an increase in the degree of opening of pores and fractures along which gases migrate to the surface [5, 8].

The fault ranking influences remarkably the size of the related radon anomaly. The parameter H varies quite broadly for faults of the same rank. However, its average values, as well as the length of the fault, become two times higher (431 m for disjunctives of the first rank and 825 m for faults of the second rank). With increasing fault rank and, consequently, the width of the radon anomaly, its contrast remains on the same level ($K_Q = 3.8\text{--}3.9$), as is evident from the average values. Moreover, the selection of strike-slip faults without the influence of the dynamic environment shows not only an decrease in K_Q (4.4 for rank 1 and 3 for rank 2), but a decrease in the intensity of anomalies Q_{\max} (5080 Bq/m³ for rank 1 and 4251 Bq/m³ for rank 2).

This tendency is in the certain contradiction with the data available on the lower tectonic (and, thus, radon) activity of small faults in comparison with the large ones, since the latter may demonstrate strike-slip faults of a higher amplitude. At this stage of the study, the result obtained may be explained by the different structure of the fault zones, which, in the first approximation, may be represented by a wide band of numerous small faults (the early stages of fault formation) or by the narrow band of tectonites of the major fault (the late stages of fault formation). A significant part of the amplitude in wide scattered faults of the first type is realized due to plastic deformation, while the second type is controlled by displacement along the fault [2]. As a result, under the same conditions, K_Q and Q_{\max} are higher in the focused faults of the late evolutionary stage (Skai, Khustai-1, Gunzhin, and others) than those in the scattered disjunctives of the early evolutionary stages (Khustai-2, Sherkhai, Avdar, and others). This is indirectly supported by the absence of seismic activity or its occurrence near the fault in the first case and by scattering in the distribution of earthquake foci in the second case (Fig. 1a).

The considered influence of fault ranks, the dynamic environment of the formation, and the state of the internal structure on radon activity reflects the impact of tectonic activity on the emanation field, but the intensity of motion is the most important component, which is indirectly estimated by the spatial and temporal distribution of seismicity near the objects of study. In the spatial relation, the analysis supported the regularity established earlier [3]: the seismically active segments of the fault are characterized by higher values of the emanation anomaly parameters in comparison with the aseismic ones. In the time aspect, on the one hand, there was a threefold reduction in the intensity of the anomaly on the Emelt fault in 2011 compared to 2010; on the other hand, a similar increase in the number of earthquakes (201 in 2010 and 542 in 2011) was registered.

The correspondence of the seismic fault regime to the nature of its radon activity is established by the example of the seismic rupture formed during the

Mogod earthquake and characterized by intermediate radon activity. As is evident for the Tulet-1 profile (Fig. 1b), the lowest of the allocated anomalies corresponds to the seismic rupture, whereas the high and more intense anomalies occur in the low relief forms. This is explained by the concentration of the activity on adjacent fault structures distinctly expressed in the relief after the strong earthquake.

CONCLUSIONS

In general, an analysis of the spatial and temporal distribution of seismic and radon activity of faults performed for the Ulaanbaatar and Mogod areas provides evidence for their close interrelation. This, together with the influence of the rank, structure, and dynamic situation of the formation of fault zones on the radon concentration in the soil, allows us to conclude that the emanation activity of faults in geodynamically active regions of Central Mongolia reflects their integral tectonic activity. However, estimation of the displacement intensity, a practically important element of tectonic activity in direct relation to the intensity and contrast of the near-fault radon anomaly, is complicated by the influence of other components of the tectonic activity. Thus, under the same conditions, higher K_Q values are typical of normal and strike-slip faults in comparison with thrusts, larger faults in relation to small ones, and, finally, for concentrated faults

of late evolutionary stages of development in comparison with the wide zones of faults at the early stages of formation of the internal structure.

REFERENCES

1. T. Sh. Dalatkazin, Yu. P. Konovalova, and V. I. Ruchkin, *Litosfera*, No. 3, 146–150 (2013).
2. V. A. Sankov and K. Zh. Seminsky, *Izv. Vyssh. Uchebn. Zaved., Geol. Razved.*, No. 4, 10–18 (1988).
3. K. Zh. Seminskii, A. A. Bobrov, S. Demberel, et al., *Izv. Sib. Otd. Sekts. Nauk Zemle Ross. Akad. Estestv. Nauk*, No. 6 (49), 68–81 (2014).
4. K. Zh. Seminsky, S. Demberel, and D. Mungunsuren, *Dokl. Earth Sci.* **474** (1), 511–516 (2017).
5. V. I. Utkin and A. K. Yurkov, *Russ. Geol. Geophys.* **51** (2), 220–227 (2010).
6. M. Bano, N. Tsend-Ayush, A. Schlupp, et al., in *Proc. Int. Conf. on Astronomy and Geophysics in Mongolia* (Mongol Altay Print., Ulaanbaatar, 2017), pp. 137–142.
7. A. Bayasgalan and J. Jackson, *Geophys. J. Int.* **138**, 784–800 (1999).
8. P. Richon, *Radiat. Meas.* **45**, 211–218 (2010).
9. K. Zh. Seminsky and S. Demberel, *Radiat. Meas.* **49**, 19–34 (2013).
10. J.-P. Toutain and J.-C. Baubron, *Tectonophysics* **304**, 1–27 (1999).

Translated by A. Bobrov